water

MDPI

Article

Assessment of Water Quality Using Chemometrics and Multivariate Statistics: A Case Study in Chaobai River Replenished by Reclaimed Water, North China

Yilei Yu [1,2], Xianfang Song [3,*], Yinghua Zhang [3] and Fandong Zheng [4]

1 Institute of Wetland Research, Chinese Academy of Forestry, Beijing 100091, China; yuyilei1222@126.com
2 Beijing Key Laboratory of Wetland Services and Restoration, Beijing 100091, China
3 Key Laboratory of Water Cycle and Related Land Surface Processes, Institute of Geographic Sciences and Natural Resources Research, Chinese Academy of Sciences, Beijing 100101, China; zhangyinghua@igsnrr.ac.cn
4 Beijing Water Science and Technology Institute, Beijing 10048, China; zfd@bwsti.com
* Correspondence: songxf@igsnrr.ac.cn; Tel.: +86-010-6488-9849

Received: 3 August 2020; Accepted: 10 September 2020; Published: 12 September 2020

Abstract: Dry rivers could be effectively recovered by reclaimed water in North China, while river water quality would be an important issue. Therefore, it is important to understand the spatiotemporal variation and controlling factors of river water. Water samples were collected during March, May, July, September, and November in the year 2010, then 20 parameters were analyzed. The water environment was oxidizing and alkaline, which was beneficial for nitrification. Nitrate was the main nitrogen form. Depleted and enriched isotopes were found in reclaimed water and river water, respectively. Total nitrogen (TN) and total phosphorus (TP) of reclaimed water exceed the threshold of reclaimed water reuse standard and Class V in the surface water quality criteria. Most river water was at the severe eutrophication level. The sodium adsorption ratio indicated a medium harmful level for irrigation purpose. Significant spatial and temporal variation was explored by cluster analysis. Five months and nine stations were both classified into two distinct clusters. It was found that 6 parameters (chloride: Cl^-, sulphate: SO_4^{2-}, potassium: K^+, sodium: Na^+, magnesium: Mg^{2+}, and total dissolved solids: TDS) had significant upward temporal variation, and 12 parameters (dissolved oxygen: DO, electric conductivity: EC, bicarbonate: HCO_3^-, K^+, Na^+, Ca^{2+}, TDS, nitrite-nitrogen: NO_2-N, nitrate nitrogen: NO_3-N, TN, TP, and chlorophyll a: *Chl.a*) and 4 parameters (Mg^{2+}, ammonia nitrogen: NH_3-N, and the oxygen-18 and hydron-2 stable isotope: $\delta^{18}O$ and δ^2H) had a significant downward and upward spatial trend, respectively. The Gibbs plot showed that river water chemistry was mainly controlled by a water–rock interaction. The ionic relationship and principal component analysis showed that river water had undergone the dissolution of carbonate, calcite, and silicate minerals, cation exchange, a process of nitrification, photosynthesis of phytoplankton, and stable isotope enrichment. In addition, gypsum and salt rock have a potential dissolution process.

Keywords: water chemistry; river water; reclaimed water; multivariate statistics; Chaobai River

1. Introduction

North China has been facing serious water resources shortage in recent decades, as a result of continual drought, large consumption of water resources, water pollution, and economic development [1,2]. The groundwater table continued to decline and many rivers have been cut off or dried up for years [3]. Beijing as the capital of China, i.e., a big city located in North China, has also been facing massive water shortage. Multi-year average precipitation and evaporation are about 590 mm and 1800 mm, respectively [4,5]. Surface water resources of Beijing was 7.22×10^8 m^3,

and 14.32×10^8 m^3 in the year 2010 and 2018, respectively [4]. In 2018, the inflow to Beijing from the middle route of the South-to-North Water Diversion Project was 11.92×10^8 m^3. Consumption of Beijing water resources was 35.2×10^8 m^3 and 39.3×10^8 m^3 in 2010 and 2018, respectively. Then, the shortage gap was satisfied by excessive use of groundwater. At the same time, utilization of reclaimed water rapidly increased from 2010 (6.8×10^8 m^3) to 2018 (10.8×10^8 m^3) [4,5]. Now, reclaimed water has become the "stable second water source of Beijing", which was used for industry reuse, agricultural irrigation, river and lake landscape, and municipal utility [6]. As reclaimed water originated from treated wastewater, water quality was significantly different from natural surface water. High and complex content of salinity, nutrients (nitrogen and phosphorus), metals, and organic matter were remarkable features of reclaimed water. This could lead to soil salination [7], accumulation of heavy metals [8], groundwater pollution risk [9,10], antibiotics risk [11], and nutrient load in surface water [12].

Therefore, an understanding of water quality is very important for better use of reclaimed water. At present, chemometrics and multivariate statistics could provide powerful exploration for revealing water chemistry/quality characteristics. The Gibbs plot was depicted by drawing the relationship of the major ion ratio vs. total dissolved solids (TDS) of water, which included major rivers, rainfall, and seawater in the world [13]. It was powerful to determine the controlling mechanisms, which contained natural processes (atmospheric precipitation, rock weathering, and evaporation–crystallization) and anthropogenic activities [14]. A complex interaction among lithosphere, atmosphere, hydrosphere, and biosphere usually caused lithological weathering, which was the source of river water chemistry [14–16]. Stoichiometric analysis, e.g., the relationship of different combinations of dissolved cations and anions, could provide qualitative sources of ions in river water, such as evaporites, carbonates, and silicates [17–19]. Multivariate statistical analyses are particularly useful to explore the water chemistry/quality data set. Correlation analysis is powerful to interpret the relationship of water quality data and to infer specific water chemical processes [20]. The inner characteristics and distribution rule of water quality could be explored using a cluster analysis, and the similarity and dissimilarity also can be clarified. It usually contains a cluster of water chemical variables and samples. Consequently, ionic transformation and spatiotemporal variation could be clearly delineated [21,22]. Analysis of variance can be used to identify whether the difference of water parameters is significant, furtherly the spatiotemporal variation could be ascertained quantificationally [23]. Water quality has an extent of random and uncertainty, which will increase the difficulty of understanding the data. By dimensionality reduction of a large amount of data, the principal component analysis could determine the key water quality parameters, which are used to identify pollutant sources and the transforming mechanism of water chemistry [24,25]. In the past, research of river water quality mainly focused on natural rivers or rivers polluted by different sources of pollutants. Less studies were performed on rivers mainly replenished by reclaimed water. Generally, the single research method was usually applied to explore the river water quality. In this study, we try to combine the application of chemometrics and multivariate statistics methods for river water quality. So, the problem of river water quality/chemistry, e.g., the relationship of different water quality parameters, spatiotemporal variation, and evolution of water chemistry, could be quantitatively solved. Therefore, the combination of chemometrics and multivariate statistics would be more effectively to clarify the water chemical composition and governing factors. This study would provide sufficient suggestions for reclaimed water reuse and management of river water quality, even for water quality control issues of discharge from wastewater treatment plants.

For recovery of the dry Chaobai River, reclaimed water with a flow of 1.0×10^5 m^3/d, treated from Wenyu River water using membrane bioreactor technology, was moved to Chaobai River for ecological implementation. So, we researched the water quality of reclaimed water and river water for better use of reclaimed water. The main objectives of our study are (1) to understand the physical and chemical composition of reclaimed water and river water; (2) to clarify the spatial and temporal variation of

water parameters; and (3) to ascertain the governing factors of water chemical evolution in the Chaobai River replenished by reclaimed water.

2. Materials and Methods

2.1. Study Site

The study site, located on the northeast of Beijing city, is the water course in Shunyi County, belonging to Chaobai River (Figure 1). The climate here has a seasonal temperature with a semi-humid monsoon climate with four distinct seasons. The multi-annual average temperature, annual rainfall, and evaporation are 11.8 °C, 614.9 mm, and 1175 mm, respectively. Meanwhile, the precipitation was concentrated mostly from June to September [26].

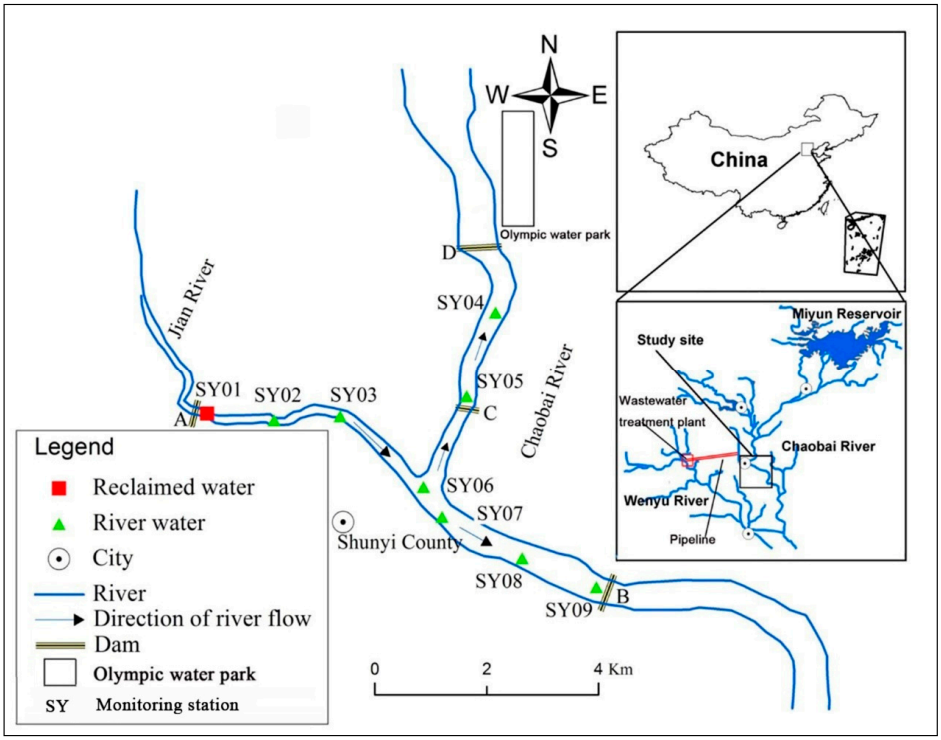

Figure 1. Location of the study site and distribution of monitoring stations.

Chaobai River has been dry as a result of continual dry weather and the impoundment of the Miyun Reservoir since 1999, which belongs to the Quaternary Holocene alluvial–diluvial strata. The riverbed is mainly composed of fine sand, silt, and gravel layers. The thickness of the sand layer is generally from ten to a few dozen meters. Floodplain and terraces on both banks of the river channel are loam and sand [26]. While, Wenyu River (Figure 1) near the Chaobai River always has water flow throughout the year, which is mainly composed of domestic wastewater from surrounding communities. Wastewater in Wenyu River was treated using membrane bioreactor technology (MBR). Consequently, treated wastewater (reclaimed water) was transported to the Jian River (length: 4 km and width: 50–90 m; tributary of Chaobai River) by a water pipeline since the year 2007 [27]. Then, the Chaobai River channel from dam B to dam D was replenished by reclaimed water with a flow of 2.5 m^3/s. Meanwhile, river flows freely through dam C. Most reclaimed water was stored in this section of the river as a result of the dams, except for evaporation and infiltration. The main channel of the river has a length of 7.3 km, width of 200–400 m, and average water depth of 2.5 m. River water flow was also changed by the dams after the replenishment of reclaimed water. One direction was the original river flow, i.e., southeast (to SY09), the other was northeast (to SY04; Figure 1).

2.2. Methods

2.2.1. Water Sampling

For investigating the water quality and controlling factors of river water replenished by reclaimed water in the Chaobai River, samples of reclaimed water and river water along the river channel were collected during March, May, July, September, and November in 2010. Nine monitoring stations (SY01–SY09) are shown in Figure 1, which included one reclaimed water and eight river water stations. In addition, one sample of reclaimed water in March was missed. Sample bottles with different volumes (100 mL and 500 mL) were made of polyethylene. The bottles were cleaned once with detergent, then cleaned once with tap water, and finally cleaned with deionized water 3 times. Water samples were collected at a depth of 50 cm below the river water surface using a plexiglass water collector. Three bottles of the water sample were collected for each monitoring station every time. The polyethylene bottles were prerinsed with water samples three times, before the final water sample was collected. The sampling frequency was five times for one year, and the sampling time was from 9:00 am to 5:00 pm. Three bottles of samples were collected at each station. The 100 mL sample was used for the determination of water stable isotopes, and the cap of the bottle was sealed with tape to prevent evaporation. A sample of 500 mL for the determination of anions, cations, nitrogen, and phosphorus was used and another sample of 500 mL was used for chlorophyll a (*Chl. a*) determination. All samples were stored in a portable cooler containing ice packs under 4 °C.

The precipitation data was measured using the tipping bucket automatic rain sensor (CG-04-D1, Hebei Yiqing Electronic Technology Company, Handan, China) on the roof of the Geographical Science Museum of the Institute of Geographical Sciences and Natural Resources Research, Chinese Academy of Sciences (40°00′11″ N, 116°23′07″ E, 45 m above sea level, about 10 m above the ground) from January to December 2010. This sampling point was 28 km from the study area in a straight line. A total of 17 precipitation events were collected, with a total precipitation of 412.7 mm. Then, monthly distribution data of precipitation in 2010 was obtained by accumulating precipitation events into the month.

2.2.2. Analytical Techniques

pH, water temperature (T, °C), dissolved oxygen (DO), and electric conductivity (EC) were measured by the portable multi-parameter water quality analyzer (American Hach HQ-40d), which was produced by HACH Company (Loveland, CO, USA). Water samples were taken back to the laboratory under 4 °C cold storage and analyzed within 24 h. The bicarbonate (HCO_3^-) was determined by titration under the addition of sulfuric acid (0.02 mol/L), which the endpoint of titration had methyl orange as an indicator. Before further ionic analysis, water samples were filtered through a 0.45 μm Millipore membrane. Major cations including potassium (K^+), sodium (Na^+), calcium (Ca^{2+}), and magnesium (Mg^{2+}) were measured by inductively coupled plasma spectroscope (ICP-OES Optima 5300DV), produced by Perkinelmer Instruments Co., LTD (Norwalk, Connecticut, USA), with a detection limit of 0.01 mg/L. Major anions including chloride (Cl^-), sulphate (SO_4^{2-}), and nitrate (NO_3^-) were measured by ion chromatograph (Thermo Fisher ICS2100) produced by the DIONEX company (Sunnyvale, CA, USA), and the detection limit was 0.01 mg/L. Ammonia nitrogen (NH_3-N), nitrite nitrogen (NO_2-N), total nitrogen (TN), and total phosphorus (TP) were measured using AMS's Smartchem 200 batch analyzer produced by Alliance company (Paris, France), with a detection limit of 0.01 mg/L. Stable isotopes (δ^2H and $\delta^{18}O$) were measured by a laser spectroscopic instrument (LGR DLT-100, Los Gatos Research, Mountain View, CA, USA), with the standard of Vienna standard mean ocean water (VSMOW). The precisions of $\delta^{18}O$ and δ^2H were 0.2‰ and 0.6‰, respectively. TDS was measured by the gravimetric method. The filtered water sample (200 mL) was placed in an evaporating dish weighed to a constant weight, and then baked to a constant weight at 103 ~ 105 °C. The TDS value was calculated by the increased weight [28]. The collected chlorophyll a (*Chl. a*) sample samples were stored at 4 °C, and 1 mL of 1% magnesium carbonate suspension was added to each liter of water

samples to prevent pigmentation caused by acidification. In the laboratory, samples were filtered and concentrated, and the filter membrane was fully grinded and extracted, then dissolved in acetone to a constant volume, and finally the supernatant was measured by spectrophotometry. These experimental details were referred from the analytical book [28].

2.3. Data Processing

Data of the major ions need to be balanced with an error of less than 5% before further analysis. The summary statistics (e.g., mean, max, min, and coefficient of variation) of water chemistry were performed by the descriptive statistics package in SPSS 16.0 software (International Business Machines Corporation, Armonk, NY, USA) [29]. Analysis of variance (ANOVA), hierarchical cluster analysis (HCA), and principal component analysis (PCA) were all performed by SPSS [29]. Analysis of variance needs two assumptions about the data, which includes normal distribution and homogeneity of variance, respectively. These two parameters could be judged by the coefficients of skewness and Kurtosis, and Levene. The data could be considered to obey the hypothesis of normal distribution and homogeneity of variance, if the p value was more than 0.05 ($p > 0.05$). PCA is a way of selecting factors belonging to the factor analysis. Whether the data are suitable for factor analysis, it could be identified by KMO (Kaiser–Meyer–Olkin) and its significance (sig.) level test. If the KMO test value is greater than 100 and $p < 0.05$, then PCA could be performed. Respect to hierarchical clustering, especially for R-type, the data need to be standardized for avoiding the difference of dimension and orders of magnitude for variables [29]. The normality of water quality data was checked firstly by SPSS 16.0 software [29]. Then, all the data (except pH) were log-transformed and standardized before further analysis [30,31].

In addition, index, i.e., $\overline{R^2}$ was used for judging the selection of key variable in HCA, that was calculated as follows:

$$\overline{R^2} = \frac{\sum \mathrm{r}^2}{m-1} \quad (1)$$

where, r^2 represents the correlation coefficient between different variables in clusters, and m represents the number of variables in one cluster.

Meanwhile, PHREEQC (Version 3, United States Geological Survey) is a hydrogeochemical simulation software based on C language [32]. It is mainly used to solve the analysis of chemical components, solute transport, and dynamic chemical reactions in the interaction system of water, gas, and rock–soil. The saturation index (SI) of major minerals was calculated by PHREEQC software.

Excessive sodium and salinity in irrigation water would result in sodium hazard. Calcium and magnesium in soil could be replaced by sodium, which leads to the reduction of permeability and soil harden [33]. Sodium adsorption ratio (SAR) calculated based on chemical variables was used to assess irrigation water quality, which was an effective evaluation index [34].

$$SAR = \mathrm{Na}^+ / \sqrt{(Ca^{2+} + Mg^{2+})/2} \quad (2)$$

where, ionic concentrations are expressed in milliequivalent per liter (meq/L).

3. Results and Discussion

3.1. Water Chemical Composition

Physical and chemical compositions of water samples in the Chaobai River are given in Table 1. pH ranged from 7.65 to 9.45, with an average value of 8.37, which showed reclaimed water and river water were all alkaline. The average value in river water was higher than that in reclaimed water. Water temperature was mainly controlled by the operation of the wastewater treatment plant (WWTP) and air temperature of seasonal variation. Electric conductivity (EC) and TDS were the similar parameters indicating the total dissolved solids in aqueous solution, which in reclaimed water were

both slightly higher than in river water. The order of nitrogen forms in reclaimed water and river water was: NO_3-N > NO_2-N > NH_3-N, and NO_3-N > NH_3-N > NO_2-N, respectively. The coefficient of variation (C.V.) of NH_3-N and NO_2-N was much higher than others. It indicated that they were prone to chemical transformation in the water environment. Considering the average, higher percentage of NO_3-N /TN in reclaimed water (85%) and river water (78%) indicated nitrate was the major nitrogen form. The order of anions in reclaimed water was: HCO_3^- > SO_4^{2-} > Cl^-; while, the order in river water was: HCO_3^- > Cl^- > SO_4^{2-}. Whereas, the order of cations (Na^+ >Ca^{2+} >Mg^{2+} > K^+) was the same in both waters. In terms of the average, seven indicators of river water were higher than in reclaimed water, which contained pH, Cl^-, Mg^{2+}, NH_3-N, *Chl.a*, $\delta^{18}O$, and δ^2H. While, the remaining indexes were the opposite. A reduction of nutrients (NO_3-N, NO_2-N, TN, and TP) may be caused by the consumption of phytoplankton or dilution [35,36]. External input from surface runoff in the rainy season could lead to the increased content of Cl^- and Mg^{2+} [37,38]. Increased ammonia content may be caused by the mineralization of organic nitrogen [39,40]. High value of *Chl.a* indicated the reproduction of phytoplankton, e.g., alga in river water [36]. Stable isotopes ($\delta^{18}O$, δ^2H) were depleted in reclaimed water, while enriched in river water (Table 1), and the similar enrichment phenomenon was also found in Huai River [10].

Table 1. Water chemical composition of reclaimed water and river water in the Chaobai River (March–November 2010).

	Reclaimed Water					River Water				
	Min.	**Max.**	**Mean**	**SD**	**C.V. (%)**	**Min.**	**Max.**	**Mean**	**SD**	**C.V. (%)**
pH	7.65	8.21	7.93	0.25	3.16	8.08	9.45	8.81	0.41	4.68
T (°C)	6.90	28.60	21.03	9.65	45.92	1.90	29.70	17.42	10.30	59.12
DO (mg/L)	4.73	8.50	7.33	1.75	23.84	1.25	10.30	6.20	2.50	40.24
EC (μS/cm)	937	1025	982	36.88	3.75	935	1047	859	90.72	10.56
Cl^-(mg/L)	72.90	114.00	87.65	18.65	21.27	65.2	148.0	98.15	19.96	20.34
HCO_3^-(mg/L)	219.00	299.00	261.75	33.24	12.70	230	386	227.78	49.01	21.52
SO_4^{2-}(mg/L)	81.90	99.50	89.33	7.97	8.92	64.30	120.00	87.04	13.66	15.69
K^+(mg/L)	12.90	18.60	16.25	2.83	17.44	6.32	25.80	15.25	4.82	31.60
Na^+(mg/L)	80.20	108.00	94.45	11.62	12.30	57.3	135.0	88.46	17.51	19.79
Ca^{2+}(mg/L)	60.10	66.40	63.47	3.17	5.00	23.7	75.2	48.92	12.80	26.17
Mg^{2+}(mg/L)	22.60	28.60	26.00	2.71	10.42	23.3	39.9	29.10	3.43	11.80
NH_3-N(mg/L)	0.03	0.11	0.08	0.03	43.92	0.02	1.81	0.38	0.42	109.57
NO_2-N(mg/L)	0.22	0.76	0.38	0.26	67.66	0.00	0.74	0.16	0.15	91.60
NO_3-N(mg/L)	10.60	19.40	14.75	3.83	25.99	0.03	19.90	7.03	5.95	84.66
TN (mg/L)	11.50	22.10	17.18	4.47	26.01	2.30	20.00	9.62	5.29	54.94
TP (mg/L)	0.44	1.52	1.05	0.46	43.8	0.09	2.76	0.60	0.55	92.00
Chl.a (μg/L)	0.50	3.58	2.03	1.77	87.03	1.96	175.00	58.87	45.18	76.74
TDS (mg/L)	568	655	601	39.35	6.55	419	794	540	80.07	14.82
$\delta^{18}O$ (‰)	−8.55	−7.25	−7.99	0.63	−7.91	−8.64	−5.14	−6.85	0.98	−14.34
δ^2H (‰)	−61.34	−55.36	−58.39	2.73	−4.68	−63.64	−43.70	−53.48	5.28	−9.86

A Pearson correlation analysis was applied to explore the relationship of water chemical parameters by SPSS, and the results are given in Table 2. Carbonate was observably positively correlated with K^+, Na^+, and Ca^{2+}, which indicated the dissolution of minerals [41]. Chloride was prominently and positively related with SO_4^{2-}, K^+, Na^+, Mg^{2+}, and TDS. TDS was significantly and positively correlated with EC, Cl^-, HCO_3^-, SO_4^{2-}, K^+, Na^+, Ca^{2+}, NO_3-N, TN, and TP, respectively. Meanwhile, the same correlation was also found between EC with these ions. It indicated these ions were the major composition of TDS and EC. While, TDS were significantly and negatively correlated with stable isotopes and *Chl.a*. This may be due to the consumption of nitrogen and phosphorus by phytoplankton [35,36]. TN was significantly and positively related with TP, indicating their common origin. At the same time, they were both significantly and positively related with EC, HCO_3^-, K^+, Na^+, Ca^{2+}, TDS, and NO_3-N. In addition, TN was also positively and negatively significantly correlated with NH_3-N and NO_2-N, respectively. TN, TP, and other cations were mainly from reclaimed water, which could explain their significant relationship. The major nitrogen forms (NO_3-N) were furtherly confirmed by its significant and positive relationship with TN (Tables 1 and 2). Part of NH_3-N will be released into the atmosphere [42–44], which could be inferred by its significant and negative relationship with TN.

Table 2. Correlation of water chemical parameters in water samples in the Chaobai River (March–November 2010).

	pH	**T**	**DO**	**EC**	**Cl^-**	**HCO_3^-**	**SO_4^{2-}**	**K^+**	**Na^+**	**Ca^{2+}**	**Mg^{2+}**	**TDS**	**NH_3-N**	**NO_2-N**	**NO_3-N**	**TN**	**TP**	***Chl.a***	**$\delta^{18}O$**	**δ^2H**
pH	1.00																			
T	0.10	1.00																		
DO	0.16	0.37 *	1.00																	
EC	−0.18	0.09	0.16	1.00																
Cl^-	0.37 *	0.00	0.11	0.10	1.00															
HCO_3^-	−0.25	0.14	0.40 **	0.66 **	0.21	1.00														
SO_4^{2-}	0.29	−0.15	−0.10	0.24	0.71 **	−0.04	1.00													
K^+	0.15	−0.08	0.38 *	0.59 **	0.59 **	0.66 **	0.51 **	1.00												
Na^+	0.11	0.06	0.27	0.70 **	0.60 **	0.59 **	0.61 **	0.93 **	1.00											
Ca^{2+}	−0.37 *	−0.04	0.42 **	0.77 **	−0.20	0.82 **	−0.16	0.51 **	0.46 **	1.00										
Mg^{2+}	0.08	0.03	0.21	−0.21	0.58 **	0.27	0.01	0.21	0.11	0.11	1.00									
TDS	−0.05	−0.06	0.31 *	0.77 **	0.49 **	0.73 **	0.43 **	0.89 **	0.89 **	0.72 **	0.20	1.00								
NH_3-N	−0.26	0.07	−0.13	−0.35	−0.20	−0.06	−0.20	−0.23	−0.24	−0.15	0.07	−0.21	1.00							
NO_2-N	−0.07	0.19	−0.02	0.45 **	−0.17	0.34 *	−0.04	0.22	0.28	0.25	−0.36 *	0.23	−0.07	1.00						
NO_3-N	−0.15	−0.20	0.24	0.85 **	0.10	0.50 **	0.20	0.64 **	0.64 **	0.75 **	−0.20 **	0.77 **	−0.41 **	0.28	1.00					
TN	−0.02	0.08	0.30	0.83 **	0.01	0.50 **	0.15	0.54 **	0.57 **	0.64 **	−0.37	0.63 **	−0.48 **	0.41 **	0.88 **	1.00				
TP	−0.14	0.30	0.33	0.77 **	0.26	0.67 **	0.22	0.56 **	0.62 **	0.62 **	−0.02	0.70 **	−0.30	0.26	0.62 **	0.67 **	1.00			
Chl.a	0.60 **	0.14	0.01	−0.44 **	0.25	−0.34 **	0.12	−0.03	−0.08	−0.53 **	0.15	−0.27	−0.09	−0.16	−0.38	−0.26	−0.29	1.00		
$\delta^{18}O$	0.33	0.31	0.01	−0.70 **	0.29	−0.28	0.09	−0.19	−0.26	−0.67 **	0.36	−0.44 **	0.26	−0.21	−0.79 **	−0.63 **	−0.41 **	0.45 **	1.00	
δ^2H	0.32	0.23	−0.03	−0.77 **	0.31	−0.39	0.13	−0.27	−0.33	−0.71 **	0.34	−0.48 **	0.30	−0.28	−0.80 **	−0.66 **	−0.46 **	0.44 **	0.94 **	1.00

*: Correlation is significant at $p < 0.05$; **: Correlation is significant at $p < 0.01$. The observation includes samples of nine stations in five months except SY01 (four months), and the numbers are 44 ($n = 44$).

Chl.a was remarkably and negatively related with EC, HCO_3^-, Ca^{2+}, $\delta^{18}O$, and δ^2H. While, it was significantly and positively related with pH. CO_2 in river water could be converted into organic matter by the photosynthesis of alga, and HCO_3^- was the carbon form in the carbonate system [45,46]. While, the consumption of nitrogen, phosphorus, and carbon would lead to the decrease of EC. In addition, the amount of O_2 produced by the photosynthesis of alga was much greater than the one required for respiration, which increased DO content in the water [47,48]. Consequently, the reduction of HCO_3^- and the increase of DO would together raise the pH value (Table 1) [49,50]. Stable isotopes were both dramatically and negatively correlated with EC, Ca^{2+}, TDS, NO_3-N, TN, and TP. Significant and positive correlation of $\delta^{18}O$ and δ^2H was determined by a stable isotope fractionation mechanism [51–53].

3.2. Spatial and Temporal Variation

3.2.1. pH, T, DO, EC, and TDS

Spatial and temporal variation of pH, T, DO, EC, and TDS is given in Figure 2. A first gradual upward and then downward trend were the clear spatial variation of pH, and the rising stage mainly occurred during stations from SY04 to SY06. The lowest pH was found in reclaimed water i.e., water sources. Moreover, pH in September was lower than in other months. Meanwhile, the pH value was very close in other months. River water received more replenishment of precipitation and surface runoff with low pH with range of 4.35–5.70 [54]. Obvious temporal variation of water temperature was found, that was mainly affected by air temperature. Its order was: July > May > September > March > November. Microbial activity was strongly influenced by water temperature. Consequently, the element cycle driven by a microbe, e.g., nitrogen would be affected by temperature variation [55]. Lower DO content was found in November, and a higher value was found in May and July (Figure 2c), while DO in other months was close. DO content varied drastically among monitoring stations. EC and TDS had the similar downward trend of spatial variation (Figure 2d,e). They both were higher in reclaimed water, and gradually decreased along the river. Furthermore, the lowest EC value (718 μS/cm) in March was found at one end of the river flow (SY04), and EC was close in different months. However, TDS in March, May, and July were slightly higher than that in September and November. Similar temporal variation of water temperature was also found in the Yongding River [56], while the spatial variation of these five parameters was different, due to the diverse water quality of reclaimed water [56] or treated wastewater [57], hydraulic conditions, and the geomorphic feature [58].

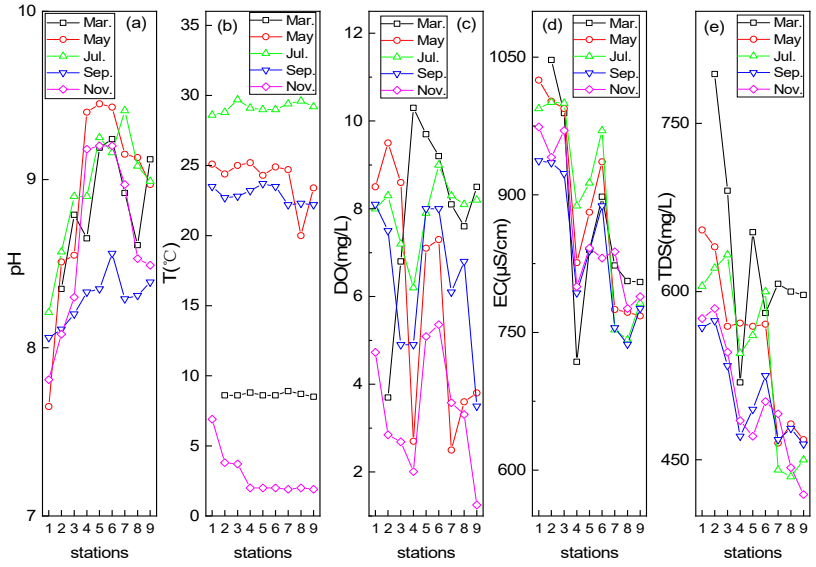

Figure 2. Spatial and temporal variation of pH (**a**), water temperature (T; **b**), dissolved oxygen (DO; **c**), electric conductivity (EC; **d**), and total dissolved solids (TDS; **e**) in the Chaobai River.

3.2.2. Major Cations and Anions

Figure 3 shows the spatial and temporal variation of major cations and anions. Cl^- has apparent temporal variation, and its order among months was: May > March > July > November > September (Figure 3a). Cl^- content increased gradually along the river water flow direction, except reclaimed water in March. Elevated chloride indicated the external input, e.g., dissolution of soil and/or sediment, or surface runoff, as chloride was the conservative ion [59]. The average value in this study was much less than the mean value in Kakoba sewage effluents (833.33 mg/L) [58]. While, the temporal variation was not significant [58]. The content of SO_4^{2-} was high in May, and low in July and September (Figure 3b). Meanwhile, it varied greatly among monitoring stations. Similar spatiotemporal variation of K^+ and Na^+ was found in Figure 3c,d. Their high values were found in March, while low values in September and November, and the medium in May and July. Their downward trend of spatial variation may be caused by ion exchange and/or dilution [19]. Variation of Ca^{2+} showed a remarkable downward spatial trend (Figure 3e). High Ca^{2+} content was firstly found in reclaimed water. However, its concentration gradually decreased along river flow, especially in SY04 and SY07 in May. The observed decrease may be the result of calcium precipitation, and/or calcium ions exchange with soils/minerals [17,60]. The content of Ca^{2+} was high in March and July, and low in May, while medium in other months. Gradual rising was the primary feature of spatial variation of Mg^{2+}, except a high value of reclaimed water in March (Figure 3f). External input and/or dissolution of mineral with magnesium may contribute to an increase [61]. High and low value of Mg^{2+} was found in March and November, respectively. While, the medium one was in other months. Major cations and anions in the river impacted by sewage effluents in the Mediterranean had significant spatiotemporal variation [57]. Complexity and high variability occurred in different rivers with diverse conditions.

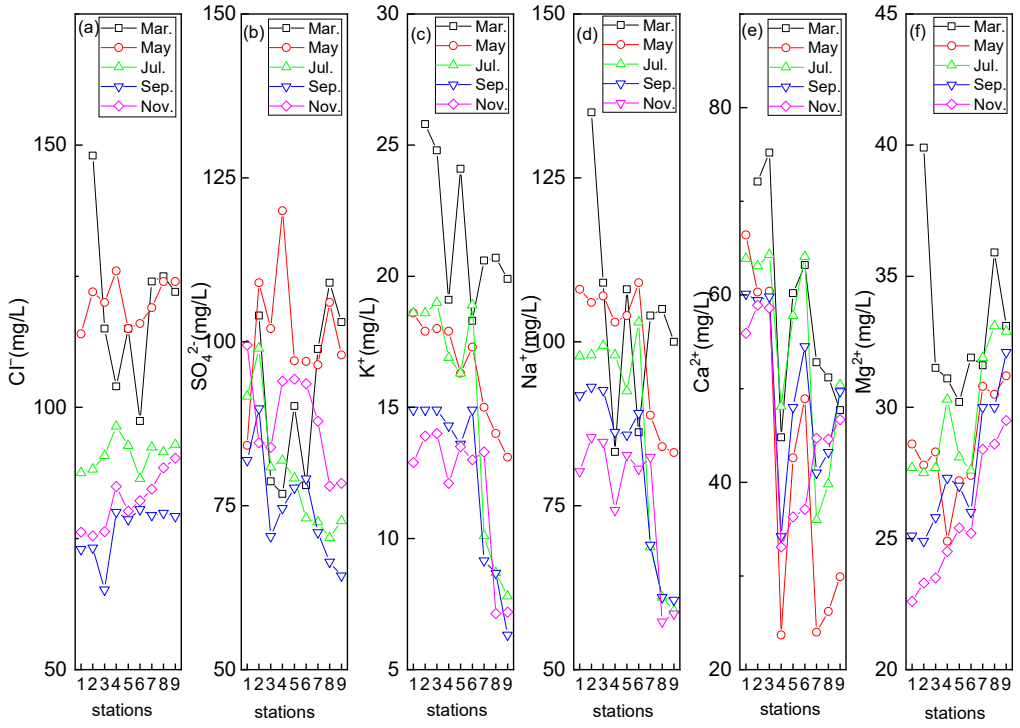

Figure 3. Spatial and temporal variation of Cl^- (**a**), SO_4^{2-} (**b**), K^+ (**c**), Na^+ (**d**), Ca^{2+} (**e**), and Mg^{2+} (**f**) in the Chaobai River.

3.2.3. Nitrogen, Phosphorus, and *Chl.a*

Spatial and temporal variations of nitrogen, phosphorus, and *Chl.a* are given in Figure 4. Spatiotemporal variation of NH_3-N was obvious (Figure 4a), with the highest and the second

highest value in SY01 (September) and SY04 (May), respectively. NH_3-N content in May and September was higher than in other months, while most values of NH_3-N were lower than 0.5 mg/L. Most NO_2-N content was lower than 0.4 mg/L (Figure 4b). Generally, spatial variation of NO_2-N was decreasing except for four peak values (SY01 and SY03 in November and SY04 and SY05 in July). These nitrogen forms also exhibited very high variability Rwizi River (Uganda) [58]. Gradual downward spatial variation of NO_3-N, TN, and TP was apparent. The evident features of NO_3-N and TN were the slight increase from SY05 to SY06 and sharp decrease in SY04. A gradual decrease was also found in the Sand River (Limpopo, South Africa) impacted by sewage effluents, and this may indicate the self-purification capacity of the river [62]. The peak value of TP was found in SY02 (May), which was higher than in reclaimed water. It may be due to the release of sediments and/or sudden external input [63,64]. While, TP in the Sand River fluctuated across the different sites [62]. First an increase and then a decrease were the feature of *Chl.a* spatial variation (Figure 4f). Meanwhile, it was higher downstream than upstream, with a peak value of SY08 in May (167 μg/L) and July (175 μg/L). High *Chl.a* was found in May and July, while a low value in November. There was a slightly low concentration of *Chl.a* in September corresponding to July, which may be caused by the dilution. Stations with a high peak value of *Chl.a* were the corresponding stations with low nitrogen and phosphorus. It further confirmed that the absorption and utilization of phytoplankton was the reason for nutrients reduction.

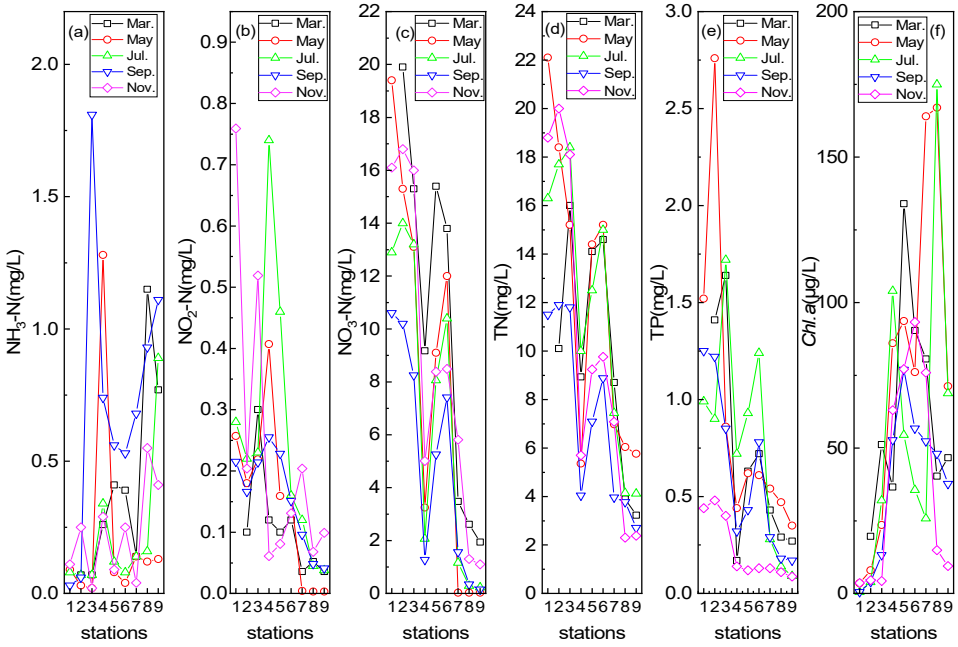

Figure 4. Spatial and temporal variation of NH_3-N (**a**), NO_2-N (**b**), NO_3-N (**c**), TN (**d**), TP (**e**), and *Chl.a* (**f**) in the Chaobai River.

3.2.4. δ^2H and $\delta^{18}O$

Figure 5 shows the spatiotemporal variation and the relationship of δ^2H and $\delta^{18}O$ in reclaimed water and river water. δ^2H and $\delta^{18}O$ had the similar variation (Figure 5a,b). The clear spatial trend was increasing variation of δ^2H and $\delta^{18}O$ from reclaimed water to the river channel end. It also indicated the enrichment process of stable isotopes, and the depleted and enriched isotopes in reclaimed water and the two ends (SY04 and SY09), respectively. Stable isotopes in March and May were higher, and gradually increased from July to November. In the dry season, e.g., March and May, high air temperature and less rainfall contributed to isotope enrichment fractionation. However, stable isotopes of river water would be prone to being depleted as a result of rainfall and surface runoff [65]. According to our observation, the precipitation in July was the largest (124.6 mm), followed by August (101.8 mm), which accounted for 30.19% and 24.67% of the annual precipitation respectively. During the rainy

season (July–September), the cumulative precipitation was 297.9 mm, accounting for 72.18%. Therefore, isotopes in November also would be affected, as it was just after the rainy season. Almost all samples were located below the global meteoric water line (GMWL) and local meteoric water line (LMWL), except several samples on and near the LMWL line (Figure 5c), which indicated that most reclaimed water and river water were influenced by strong evaporation [52]. Additionally, it was consistent with the results of the isotope enrichment feature (March and May) in Figure 5a,b. Samples located on LMWL showed their source of atmospheric precipitation and less evaporation [53,66]. The evaporation line of stable isotopes among different months were different, and the order of the slope was: July (6.13) > March (5.72) > November (5.21) > May (4.85) > September (4.02).

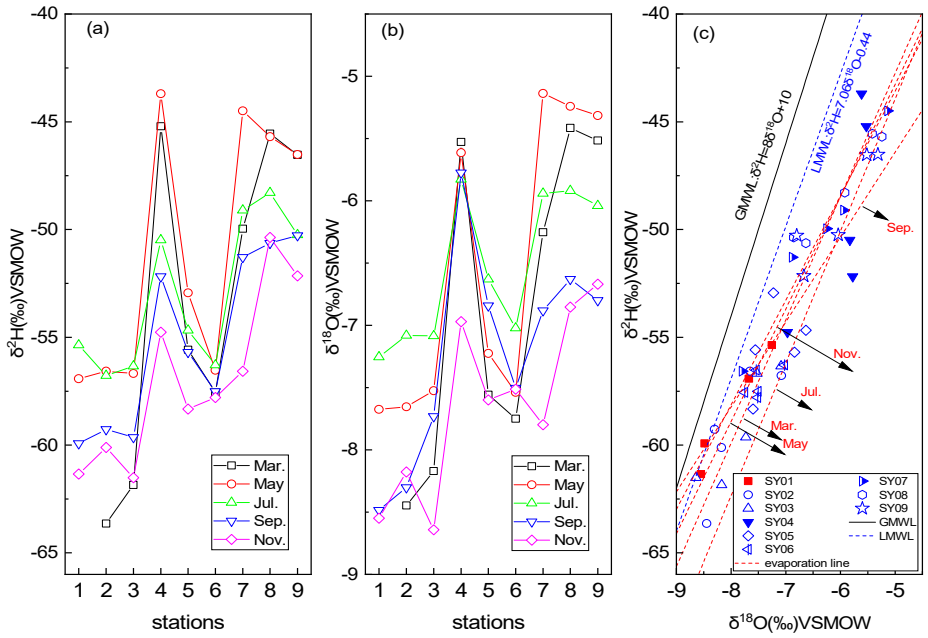

Figure 5. Spatiotemporal variation of δ^2H (**a**) and $\delta^{18}O$ (**b**), and their relationship (**c**) in the Chaobai River (GMWL (global meteoric water line) [53] and LMWL (local meteoric water line) [67] in Figure 5c were cited from published articles, respectively. Red dashed lines represent evaporation line of river water in different months).

3.3. Processes Controlling Water Chemistry

3.3.1. Gibbs Plot and Bivariate Plot

Mechanisms controlling river water chemistry included atmospheric precipitation, rock weathering, evaporation–crystallization processes [13], and anthropogenic activities [14]. The high ratio of $Na^+/(Na^+ + Ca^{2+})$, low ratio of $Cl^-/(Cl^- + HCO_3^-)$, and medium TDS concentration were found in the Gibbs plot (Figure 6). Meanwhile, distributions of reclaimed water and river water samples in cation and anion plots were both located in the rock dominance area. It indicated that river water chemistry was mainly controlled by reclaimed water or the interaction of river water with soil/rock. While, the effect of precipitation and evaporation was weak. The discharge of reclaimed water from WWTP was about 1.0×10^5 m^3/day. As a result, the TDS load was about 60.1 Ton/day, according to the average value of the TDS concentration (601 mg/L). Similar Gibbs plot results were found in the Yongding River, which was also replenished by reclaimed water [56]. Water chemistry in headwaters of the Yangtze River [15] and Yellow River [68] in China was governed by rock weathering, which was less impacted by human activities. While, evaporation–crystallization plays an important role in water chemistry in the river of an arid watershed, e.g., Northern Xinjiang, China [16].

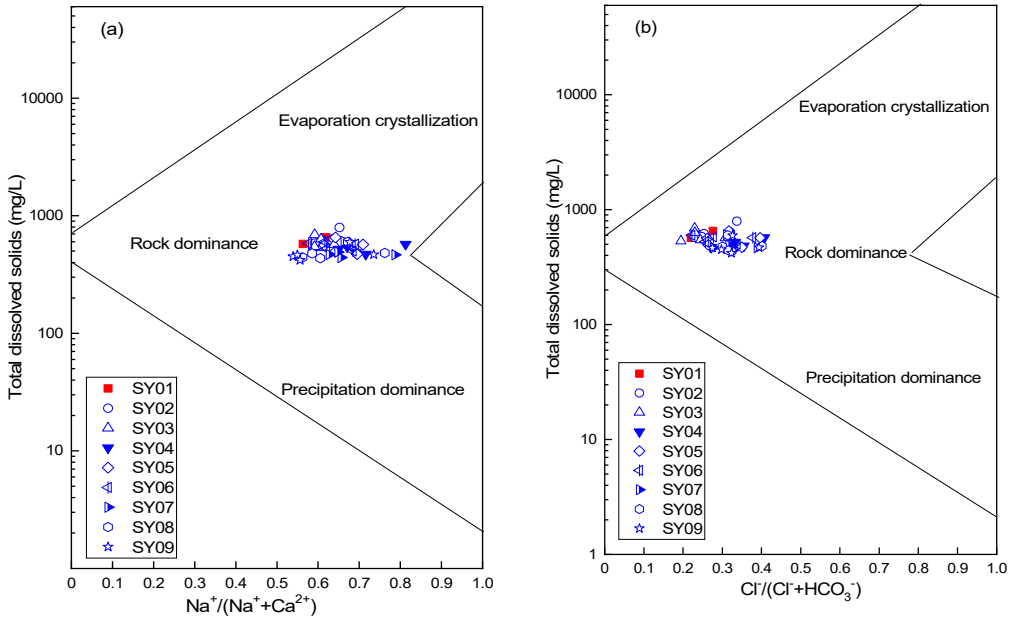

Figure 6. Gibbs graph of major cations (**a**) and anions (**b**) in the Chaobai River channel replenished by reclaimed water.

Mineral dissolution, precipitation, and redox reaction in the water environment could be inferred by the relationship of different dissolved ions in waters [13,69]. The ratio of Ca^{2+}/Mg^{2+} could indicate the dissolution of carbonate minerals [69]. The ratio value was about equal to 1, indicating the dissolution of dolomite, that included SY04 (March and July), four samples in November (SY05, SY06, SY07, and SY08), SY09 (July, September, and November; Figure 7a). The value was between 1 and 2, indicating the dissolution of calcite, which included reclaimed water (SY01), river water (SY02 and SY03) river samples of SY05 (March and May) and SY06 (Figure 7a). The ratio value of the remaining samples was less than 1, showing the decrease of Ca^{2+}, which may be caused by ion exchange. Values of $Ca^{2+}+Mg^{2+}$ vs. the cation of all reclaimed water and river water samples were located above the equilibrium line (1:1; Figure 7b). It indicated that Ca^{2+} and Mg^{2+} were mainly from the dissolution of carbonate rock and calcite [18,41]. All samples of $Na^{+}+K^{+}$ vs. Cl^{-} (Figure 7c) were located below the equilibrium line, indicating that sodium and potassium ions were also affected by the dissolution of silicate minerals except the dissolution of salt rock [68]. Samples of $Na^{+}+Ca^{2+}$ vs. HCO_3^{-} (Figure 7d) were all located below the equilibrium line, showing that sodium and calcium were more than bicarbonate, which indicated the dissolution of calcium-bearing minerals. Most of $SO_4^{2-}+Cl^{-}$ vs. HCO_3^{-} were located below the equilibrium line (Figure 7e), indicating the influence of strong evaporation. Some of $SO_4^{2-}+HCO_3^{-}$ vs. $Ca^{2+}+Mg^{2+}$ were located near the line (Figure 7e), indicating the dissolution of carbonate minerals [70]. While, most were below the line (Figure 7e), indicating the dissolution of the silicate mineral. The same silicate weathering location was found between the plot of $Ca^{2+}+/Na^{+}$ vs. Mg^{2+}/Na^{+} (Figure 7g), and plot of Ca^{2+}/Na^{+} vs. HCO_3^{-}/Na^{+} (Figure 7h), indicating the weathering and dissolution of the silicate mineral.

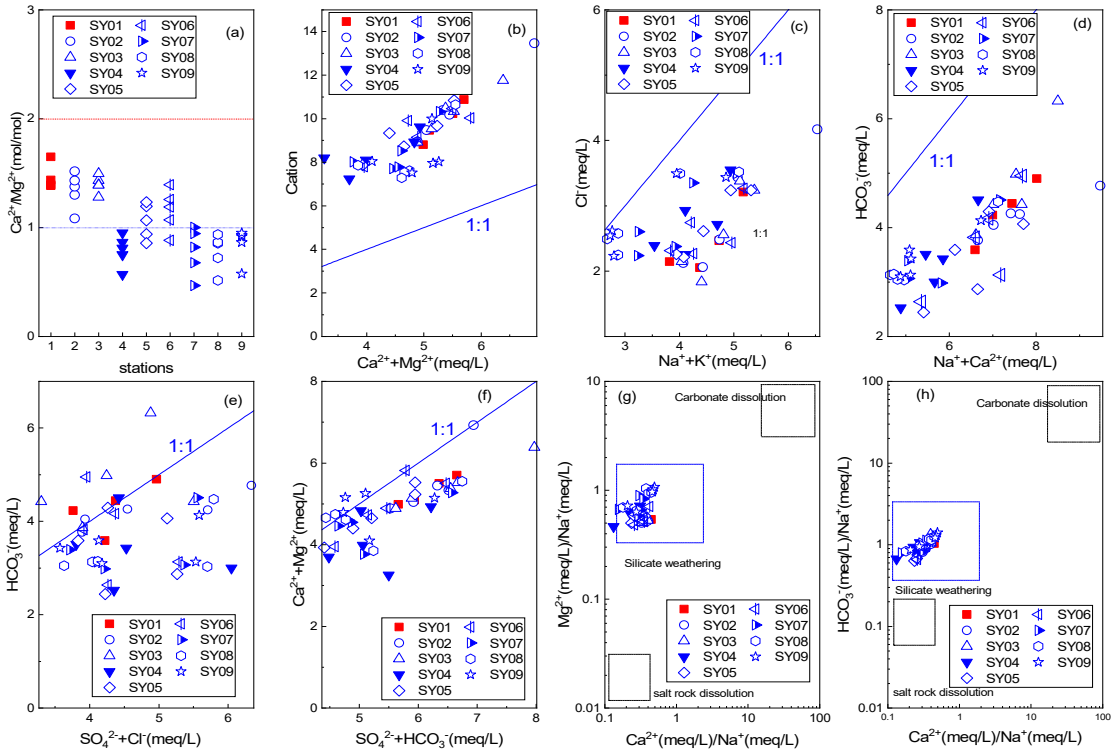

Figure 7. Plot of the ratio of Ca^{2+}/Mg^{2+} (**a**), bivariate plot of $Ca^{2+}+Mg^{2+}$ vs. the cation (**b**), $Na^{+}+K^{+}$ vs. Cl^{-} (**c**), $Na^{+}+Ca^{2+}$ vs. HCO_3^{-} (**d**), $SO_4^{2-}+Cl^{-}$ vs. HCO_3^{-} (**e**), $SO_4^{2-}+HCO_3^{-}$ vs. $Ca^{2+}+Mg^{2+}$ (**f**), $Ca^{2+}+/Na^{+}$ vs. Mg^{2+}/Na^{+} (**g**), and Ca^{2+}/Na^{+} vs. HCO_3^{-}/Na^{+} (**h**) in all samples.

Samples of $1/2HCO_3^{-} + SO_4^{2-}$ vs. $Ca^{2+} + Mg^{2+}$ were located near the equilibrium line (Figure 8a), indicating the dissolution of calcite, dolomite, and gypsum [71,72]. All samples were below the line except one sample, showing the excess $Ca^{2+}+Mg^{2+}$. These cations would be balanced by other anions, which may be silicate. Variation of the ratio of $Na^{+}/Ca^{2+}+Mg^{2+}$ (Figure 8b) was first to increase and then to decrease, which indicated the occurrence of cation exchange with clay mineral or soils [70]. Lower values were found in SY08 and SY09 stations. The process of weathering and hydrolysis of carbonate rock or silicate minerals produced equal amounts of divalent cations, HCO_3^{-} and SO_4^{2-}. As a result, $Ca^{2+}+Mg^{2+}$-HCO_3^{-}-SO_4^{2-}, and Na^{+}-Cl^{-} were used to indicate the participation of cation exchange, respectively [71]. Some samples of $Ca^{2+} + Mg^{2+}$- HCO_3^{-}-SO_4^{2-} vs. Na^{+}-Cl^{-} were located around the line ($y = -x$; Figure 8c), which indicated the clear cation exchange. Others showed the excess sodium ions from reclaimed water. In Figure 8d, the ratio of Na^{+}/Cl^{-} samples was all more than 1, except three samples (SY08 and SY09 in November and SY09 in July). The average value of Na^{+}/Cl^{-} in reclaimed water was 1.69, indicating the excess sodium. Values of Na^{+}/Cl^{-} in most river water samples were close to or less than the reclaimed water, which indicated the external chloride ion. The ratio of Na^{+}/Cl^{-} was greater than 1, indicating the possible cation exchange [73]. The downward trend of the Na^{+}/Cl^{-} value may be caused by the following reason. A higher Na^{+} content exceeded the equilibrium concentration of exchangeable cations in the medium. Then, the exchange of Ca^{2+} and adsorbed Na^{+} would be suppressed, and even reverse cations exchange would occur. Na^{+} and Ca^{2+} in the water body exchange and Mg^{2+} may also participate in the exchange [17,19].

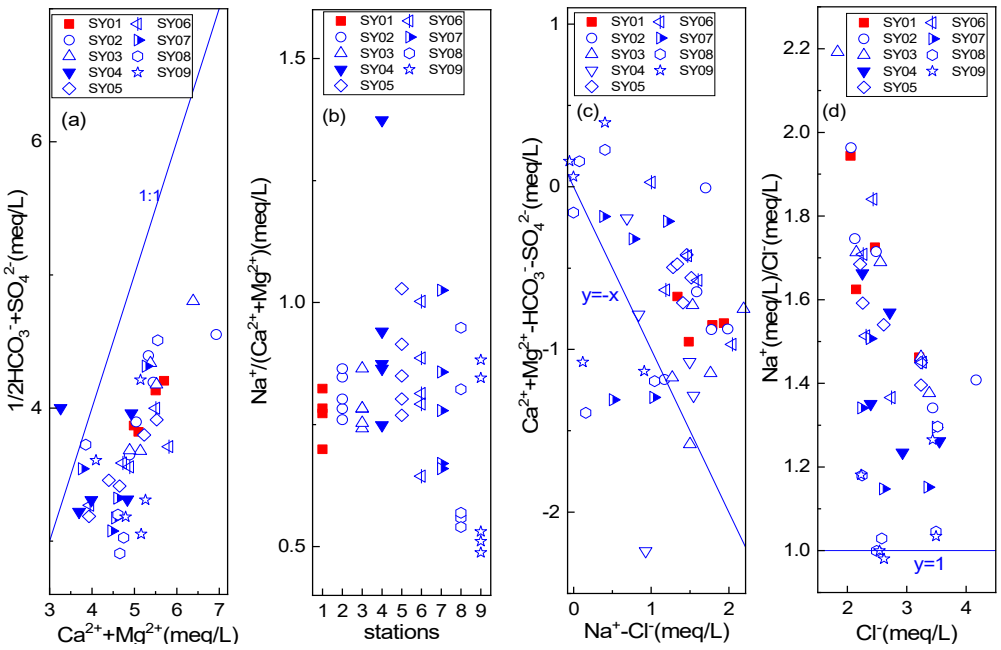

Figure 8. Plot of the ratio of Ca^{2+} + Mg^{2+} vs. $1/2HCO_3^-$ + SO_4^{2-} (**a**), Na^+/Ca^{2+} + Mg^{2+} (**b**), Na^+-Cl^- vs. Ca^{2+} + Mg^{2+}- HCO_3^--SO_4^{2-} (**c**), and Cl^- vs. Na^+/Cl^- (**d**) in all samples.

Saturation index (SI) of reclaimed water and river water samples is given in Table 3. Potential dissolution and precipitation processes in the aqueous solution could be inferred by SI values. A zero SI value indicated the equilibrium state of the mineral to the aqueous, and a positive value showed the supersaturated state, while a negative value indicated the unsaturated state [32]. The SI value of gypsum ($CaSO_4$ and $CaSO_4{\cdot}2H_2O$) and halite (NaCl) was negative, while the SI value of calcite ($CaCO_3$) and dolomite (Ca Mg $(CO_3)_2$) was positive. This indicated the potential dissolution process of gypsum and salt rock, and precipitation of calcite and dolomite in reclaimed water and river water. The excessive Na^+ of water samples may require silicate dissolution to balance it.

Table 3. Saturation index (SI) of samples in monitoring stations in the Chaobai River (March–November 2010).

	SY01	SY02	SY03	SY04	SY05	SY06	SY07	SY08	SY09
$CaSO_4$	−1.99	−1.97	−2.04	−2.23	−2.13	−2.12	−2.23	−2.20	−2.17
$CaCO_3$	0.63	0.94	1.19	1.09	1.36	1.46	1.16	1.00	1.12
Ca Mg $(CO_3)_2$	1.16	1.76	2.26	2.32	2.73	2.89	2.47	2.12	2.32
$CaSO_4{\cdot}H_2O$	−1.76	−1.73	−1.81	−2.00	−1.90	−1.89	−1.19	−1.96	−1.94
NaCl	−6.68	−6.58	−6.62	−4.39	−6.62	−4.26	−6.67	−6.71	−6.72

The numbers of measurements of all monitoring stations were five, except SY01 station (n = 4).

3.3.2. Redox Condition and Nitrogen Forms

Transformation and species of nitrogen in aqueous solution were strongly impacted by the redox environment [74,75], which could be characterized by DO and/or ORP measured in the field. The corresponding relationship of DO and three nitrogen forms (NO_3-N, NH_3-N and NO_2-N) is given in Figure 9. Nitrite was usually the intermediate of the nitrification reaction, which was not stable and easy to be oxidized [76]. In Figure 9, average DO content of river water in March, May, July, September, and November was 7.99 ± 2.07 mg/L, 5.64 ± 2.79 mg/L,7.90 ± 0.85 mg/L, 6.21 ± 1.66 mg/L, and 3.27 ± 1.41 mg/L, respectively. The saturated oxygen content of water was about 10 mg/L at normal temperature and atmospheric pressure [48,77]. DO content was more than 5 mg/L except the one in

November. Additionally, the oxidizing environment contributes to nitrification [78]. The decrease in November probably was due to low temperature and less aquatic plants [49,79].

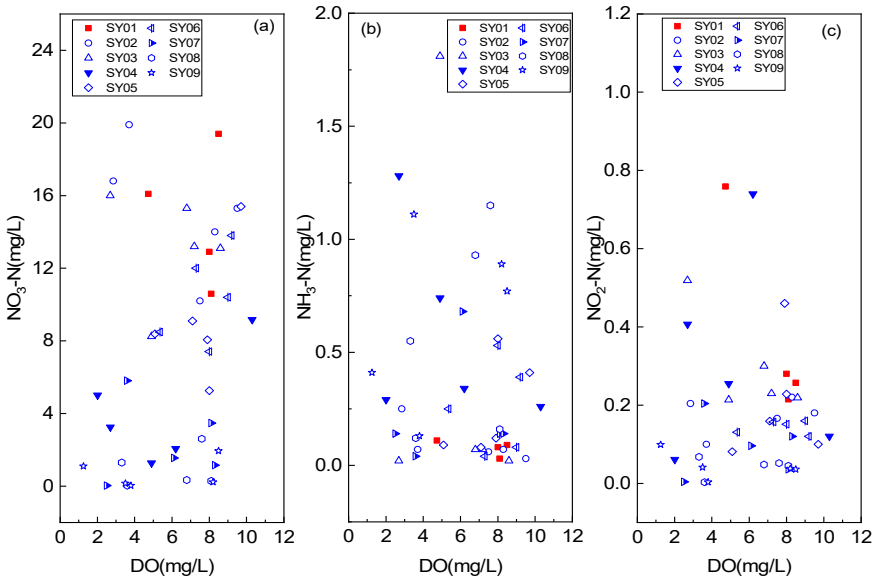

Figure 9. Relationship of DO with NO_3-N (**a**), NH_3-N (**b**), and NO_2-N (**c**) in reclaimed water and river water.

pH also played an important role in nitrogen transformation, and the double influences of pH and the redox environment could be evaluated by the pH–pE plot [78]. Therefore, samples of reclaimed water and river water were projected into Figure 10. All samples were located around the NO_3^- line, where the stable nitrogen form was nitrate (NO_3^-, +5). High DO value of reclaimed water (7.33 ± 1.75) and river water (6.20 ± 2.47) showed the oxidizing water environment, which was beneficial for nitrate stable and nitrification [78,80].

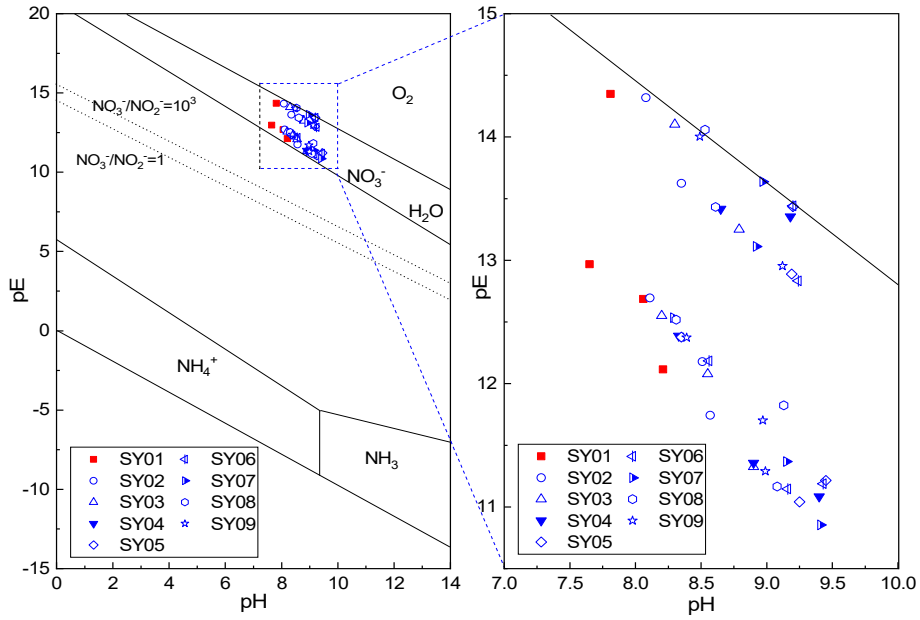

Figure 10. pH–pE diagram of reclaimed water and river water samples in the Chaobai River.

3.3.3. Cluster Analysis and Spatiotemporal Similarity

For identifying the spatiotemporal variation, the key variables should be firstly confirmed. Hence, three cluster analysis results are shown in Figure 11. In Figure 11c, twenty water chemical parameters were divided into seven clusters by the R-type cluster method for variables. Clusters were as follows. I: $\delta^{18}O$, $\delta^{2}H$, pH, and *Chl.a*; II: Mg^{2+}; III: Cl^{-}, SO_4^{2-}; IV: NH_3-N; V: T, DO; VI: K^{+}, Na^{+}, TDS, HCO_3^{-}, Ca^{2+}, NO_3-N, TN, EC, and TP; VII: NO_2-N. The R^2 value is calculated according to equation 1 if the quantity of parameters in one cluster was more than 2. The parameter with the highest R^2 value was retained for the key parameter. The R^2 value of $\delta^{18}O$ and TDS was 0.45 and 4.80, respectively. As a result, nine parameters ($\delta^{18}O$, Mg^{2+}, Cl^{-}, SO_4^{2-}, NH_3-N, T, DO, TDS, and NO_2-N) were selected as the key ones for further spatiotemporal cluster analysis. Five months were classified into two groups, Cluster I includes March and May, and Cluster II includes July, September, and November. These two distinct groups show the significant temporal variation. Spatial variation and similarity were analyzed by an HCA analysis (Figure 11c). All monitoring stations were classified into two groups, which include Cluster I (SY04, SY07, SY08, andSY09) and Cluster II (SY01, SY02, SY03, SY05, and SY06). Stations in Cluster II and Cluster I represent the upstream and downstream (Figure 1), respectively. The flow direction of reclaimed water along the river channel would eventually go in two directions, one was SY04 station and the other was SY09 station, because of the blocking effect of the rubber dam (Figure 1).

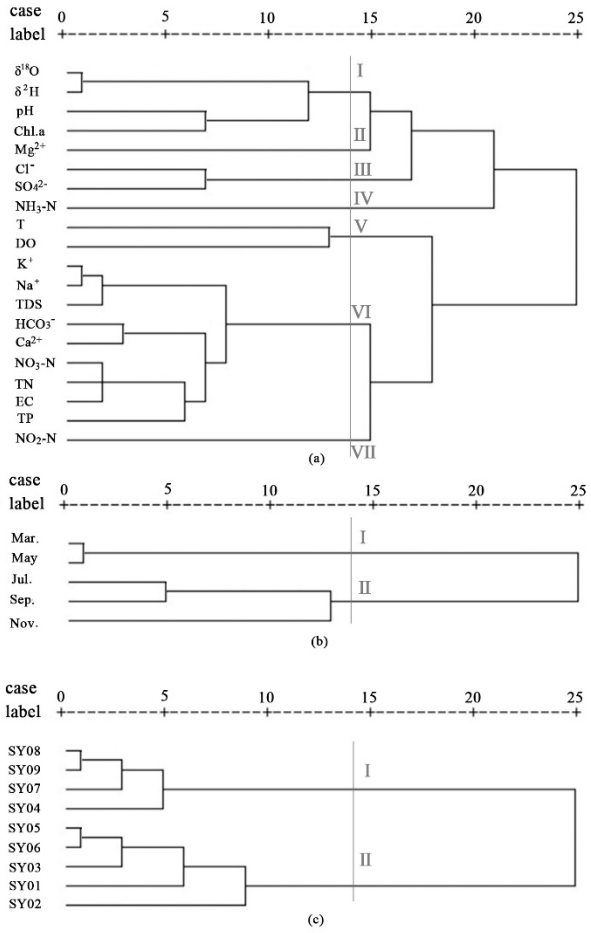

Figure 11. Cluster analysis of water quality variables (**a**), months (**b**), and monitoring stations (**c**) in the Chaobai River.

Parameters with a significant difference in different clusters were identified using an ANOVA analysis by SPSS software [29], and the corresponding results are given in Table 4. Whereas, parameters

with no significant difference were not listed. In temporal clusters, six parameters in Cluster I were significantly higher than the ones in Cluster II, which included Cl^-, SO_4^{2-}, K^+, Na^+, Mg^{2+}, and TDS. In the spatial clusters, 12 parameters in Cluster I were significantly less than in Cluster II, which included DO, EC, HCO_3^-, K^+, Na^+, Ca^{2+}, TDS, NO_2-N, NO_3-N, TN, TP, and *Chl.a*. While, four parameters in Cluster I were significantly higher than in Cluster II, which included Mg^{2+}, NH_3-N, $\delta^{18}O$, and δ^2H. As a result, the parameters with a significant difference had remarkable spatiotemporal variation. $\delta^{18}O$ and δ^2H of reclaimed water (−7.99‰ ± 0.6‰ and −58.39‰ ± 2.73‰) were more depleted than the ones in downstream stations (SY04: −5.94‰ ± 0.58‰ SY07: −49.26‰ ± 4.68‰; SY09: −6.07‰ ± 0.66‰, and SY08: −49.15‰ ± 2.51‰). The evaporation process along the river may lead to more isotope enrichment. Reclaimed water was the main source of river water, besides the precipitation and surface runoff from precipitation. Stable isotopes of precipitation were more depleted compared with reclaimed water [10]. Therefore, strong evaporation was the controlling reason for stable isotope enrichment downstream [53,66].

Table 4. Parameters in spatiotemporal clusters with a significant difference in the Chaobai River.

		Cl^-	SO_4^{2-}	K^+	Na^+	Mg^{2+}	TDS		
Temporal clusters	I	119.44 [a]	96.97 [a]	18.91 [a]	101.37 [a]	30.70 [a]	590.12 [a]		
	II	83.19 [b]	81.12 [b]	13.10 [b]	81.21 [b]	27.63 [b]	518.00 [b]		
		DO	EC	HCO_3^-	K^+	Na^+	Ca^{2+}	Mg^{2+}	TDS
Spatial Cluster	I	5.47 [b]	786 [b]	208 [b]	13.10 [b]	79.36 [b]	40.59 [b]	30.36 [a]	495 [b]
	II	7.00 [a]	940 [a]	250 [a]	17.21 [a]	97.04 [a]	58.22 [a]	27.51 [b]	588 [a]
		NH_3-N	NO_2-N	NO_3-N	TN	TP	*Chl.a*	$\delta^{18}O$	δ^2H
Spatial Cluster	I	0.51 [a]	0.124 [b]	2.04 [b]	5.33 [b]	0.281 [b]	71.00 [b]	−6.11 [a]	−49.20 [a]
	II	0.22 [b]	0.234 [a]	12.47 [a]	14.46 [a]	0.944 [a]	39.29 [a]	−7.66 [b]	−57.87 [b]

Note: Average values of the same parameters in corresponding groups with different letters are significantly different ($p < 0.05$). Temporal clusters/ Spatial Cluster

3.3.4. Principal Component Analysis and Controlling Factors

For inferring the controlling factors, two clusters were further analyzed by PCA (Table S1), and the relationship plots are given in Figure 12. The principal components would be retained according to the corresponding eigenvalue >1 [24], and the critical related parameters could be kept in terms of an explaining proportion >0.60 [25]. In Cluster I, six principal components with a total explaining 90.46% were retained. PC1 had significant and positive loading with Cl^-, SO_4^{2-}, K^+, Na^+, TDS, $\delta^{18}O$, and δ^2H. PC2 was highly and positively related with HCO_3^-, Ca^{2+}, and Mg^{2+}. PC3 had a high and positive relation with EC, NO_2-N, and TP. High and positive loading with these three components showed main water chemical composition of TDS and EC, and mineral dissolution. PC4 had high and positive loading with $\delta^{18}O$ and δ^2H. PC5 was positively related with Na^+, TN, and *Chl.a*, while negatively related with NH_3-N. PC6 was highly and positively related with NO_3-N and TN. NO_3-N was the main nitrogen formation formed by nitrification of NH_3-N [78]. As a result, the negative loading with NH_3-N could be found. Meanwhile, nitrate was also the nitrogen consumed by phytoplankton [35]. Therefore, PC5 and PC6 mainly indicated the nitrogen transformation and the photosynthesis by phytoplankton. In Cluster II, five principal components explaining 87% were retained. PC1 had high and positive loading with EC, Cl^-, HCO_3^-, K^+, Na^+, Ca^{2+}, Mg^{2+}, and TDS, which indicated reclaimed water was the main source of major ions. Additionally, these stations were strongly impacted by reclaimed water. PC2 was highly related with *Chl.a*, $\delta^{18}O$, and δ^2H. PC4 had a negative loading with SO_4^{2-}. There were no highly related parameters to PC3 and PC5. High and positive loading of $\delta^{18}O$ and δ^2H, e.g., PC1, PC4 of Cluster I, and PC2 of Cluster II together showed that stable isotope compositions were controlled by reclaimed water (main water source) and strong evaporation.

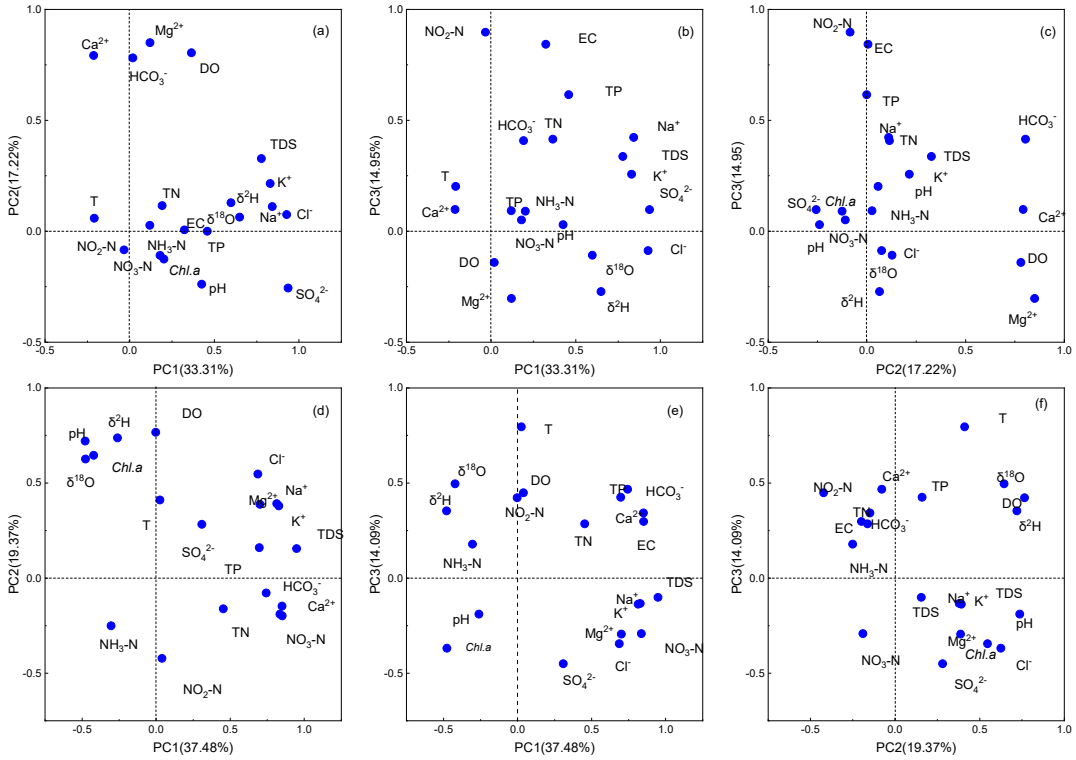

Figure 12. Relationship of principal components in spatial cluster I (**a**–**c**) and II (**d**–**f**).

Nitrogen and phosphorus are the nutrient elements for phytoplankton growth. Consequently, N and P contents would be affected by the biomass of phytoplankton [49]. Therefore, the relationship of nutrients with *Chl.a* were complicated. Sometimes, a significant and positive correlation in a certain period and a disproportionate relationship both could be found in the water environment [35,81]. There must be a relatively excessive amount of N (for P-restricted water) or P (for N-restricted water). Nutrients would be generally consumed by phytoplankton according to the Redfield ratio [82,83]. This case could be identified by the ratio of N/P. As a result, the surplus nutrient would not contribute to eutrophication. In fresh water, the N/P ratio was less than 7, indicating that N was the possible restrictive nutrient, and if the N/P ratio was greater than 7, then P was the possible restrictive one. Except SY02 in May, the ratio values of all monitoring stations were much higher than 7. Therefore, P was the restricted nutrient. Besides, hydrodynamic conditions such as temperature, light, water volume, and flow rate were also important influencing factors [49,81].

3.4. Assessment of Water Quality

According to the water quality standard for reclaimed water used for a scenic environment (GB/T18921-2019) in China [84], the average pH of reclaimed water (Table 1) was 7.93 ± 0.25, which was in the range of 6–9; the means of NH_3-N, TN, and TP were 0.08 ± 0.03 mg/L, 17.18 ± 4.47 mg/L, and 1.05 ± 0.46 mg/L, respectively. Correspondingly, their threshold values were 5 mg/L, 15 mg/L, and 0.5 mg/L. Therefore, TN and TP of reclaimed water should be reduced to meet the current standard requirement [84]. In terms of the surface water environment quality standard (GB3838-2002) in China [85], Class I is for the source of drinking water, the National Nature Reserve; Class II is for the centralized drinking water surface water source with the first level protected areas, rare aquatic habitat; and Class V is for the agricultural water area and the general landscape requirements of the waters. Average value of TN (9.62 ± 5.29 mg/L) and TP (0.60 ± 0.55 mg/L) in river water exceeded their limited value of the V class (2.0 mg/L, 0.4 mg/L). While, NH_3-N (0.38 ± 0.42) in river water was in the range of the I (0.15 mg/L) and II (0.50 mg/L) class, and DO (6.20 ± 2.50 mg/L) was higher than the threshold value in the II (6.00 mg/L) class.

On the basis of the sodium adsorption ratio (SAR), proposed by Richards [86], levels were divided into four classes (S1: <40; S2: 40–90; S3: 90–150; and S4: >150), and the corresponding harmful extents were low, medium, high, and very high, respectively. SAR of reclaimed water and river water were 57.80 ± 5.43 and 56.84 ± 10.27, respectively. Both were in the range of 46.46 ± 12.66–62.02 ± 6.92. As a result, the level was S2, indicating a medium harmful level. TP = 0.02 mg/L and TN = 0.2 mg/L, which were the internationally recognized threshold for eutrophication [87]. TP and TP in reclaimed water and river water were significantly higher than these threshold values. *Chl.a* in almost all samples were higher than 40 μg/L, except for three monitoring stations (SY01, SY02, and SY03) and some individual samples (SY04 in March; SY06 and SY07 in July; SY09 in September and November; and SY08 in November), which indicated severe eutrophication [87,88]. Except for SY01 and SY02, the remaining samples were at the eutrophication level, with *Chl.a* > 7 μg/L.

4. Conclusions

Chemometrics and multivariate statistics were used to study the characteristics and controlling factors in Chaobai River water, replenished by reclaimed water. The main conclusions were as follows. All water was oxidized and alkaline, which was beneficial for nitrification. Nitrate was the main nitrogen form in reclaimed and river water. Depleted and enriched stable isotopes were in reclaimed water and river water, respectively. TN and TP of reclaimed water exceeded the threshold of the reclaimed water reuse standard and Class V in the surface water quality criteria. Most river water was at the severe eutrophication level. The sodium adsorption ratio indicated a medium harmful level for irrigation purposes. Significant spatial and temporal variation was explored by a cluster analysis. Five months are classified into two distinct groups (I: March, May; II: July, September, and November). Nine stations were classified into two clusters (upstream: SY01, SY02, SY03, SY05, and SY06 and downstream: SY04, SY07, SY08, andSY09). Six parameters (Cl^-, SO_4^{2-}, K^+, Na^+, Mg^{2+}, and TDS) had significant upward temporal variation. Twelve parameters (DO, EC, HCO_3^-, K^+, Na^+, Ca^{2+}, TDS, NO_2-N, NO_3-N, TN, TP, and *Chl.a*.) had a significant downward spatial trend. While, four parameters (Mg^{2+}, NH_3-N, $\delta^{18}O$, and δ^2H) were the opposite. The Gibbs plot showed that river water chemistry was mainly controlled by reclaimed water or the interaction of river water with soil/rock. The ionic relationship and principal component analysis showed that river water had undergone the dissolution of carbonate, calcite, and silicate minerals, cation exchange, a process of nitrification, photosynthesis of phytoplankton, and stable isotope enrichment by strong evaporation, and gypsum and salt rock have a potential dissolution process, after reclaimed water was replenished to the river. We think that water quality of reclaimed water should be furtherly improved to avoid river water eutrophication, especially for nitrogen and phosphorus.

Supplementary Materials: The following are available online at http://www.mdpi.com/2073-4441/12/9/2551/s1, Table S1: Principal component analysis of spatial clusters including Group I and Group II.

Author Contributions: Y.Y. and X.S. had the original idea for the study, and carried out the design with all authors. F.Z. and Y.Z. had collected water samples in field and participate laboratory analysis. Y.Y. drafted the manuscript, and other authors gave advices. All authors have read and agreed to the published version of the manuscript.

Funding: This research was funded by the Government Funded Abroad Program (CAFYBB2019GC001-22) and the Basic Research Project (CAFYBB2017ZA007) of Chinese Academy of Forestry and the National Natural Science Foundation of China (41601037).

Acknowledgments: We wish to thank the two anonymous reviewers for their invaluable comments and constructive suggestions used to improve the quality of the manuscript.

Conflicts of Interest: The authors declare no conflict of interest.

References

1. Xia, J. A perspective on hydrological base of water security problem and its application study in North China. *Process. Geogr.* **2002**, *21*, 517–526. (In Chinese)
2. Xia, J.; Liu, M.; Jia, S.; Song, X.; Luo, Y.; Zhang, S. Water security problem and research perspective in North China. *J. Nat. Resour.* **2004**, *19*, 550–560. (In Chinese)
3. Wenquan, G.; Dongguo, S. Risk Evaluation of Water Shortage in Source Area of Middle Route Project for South-North Water Transfer in China. Available online: https://ideas.repec.org/a/spr/waterr/v26y2012i12p3479-3493.html (accessed on 12 September 2020).
4. Fan, Q.; Dai, L.; Liu, W.; Jiao, Z.; Jiang, T.; Bai, G.; Liu, B. *Beijing Water Resources Bulletin in 2010*; Beijing Municipal Bureau of Water Affairs; China Water Conservancy and Hydropower Press: Beijing, China, 2011. (In Chinese)
5. Zhou, Z.; Liu, W.; Tang, N.; Jiao, Z.; Li, M.; Zhao, H. *Beijing Water Resources Bulletin in 2018*; Beijing Municipal Bureau of Water Affairs; China Water Conservancy and Hydropower Press: Beijing, China, 2019; pp. 1–20. (In Chinese)
6. Yang, H.; Abbaspour, K.C. Analysis of wastewater reuse potential in Beijing. *Desalination* **2007**, *212*, 238–250. [CrossRef]
7. Mohammad, M.J.; Mazahreh, N. changes in soil fertility parameters in response to irrigation of forage crops with secondary treated wastewater. *Commun. Soil Sci. Plant. Anal.* **2011**, *34*, 1281–1294. [CrossRef]
8. Asgari, K.; Cornelis, W.M. Heavy metal accumulation in soils and grains, and health risks associated with use of treated municipal wastewater in subsurface drip irrigation. *Environ. Monit. Assess.* **2015**, *187*, 4565. [CrossRef] [PubMed]
9. Yu, Y.; Song, X.; Zhang, Y.; Zheng, F.; Liang, J.; Han, D.; Ma, Y.; Bu, H. Identification of key factors governing chemistry in groundwater near the water course recharged by reclaimed water at Miyun County, Northern China. *J. Environ. Sci.* **2013**, *25*, 1754–1763. [CrossRef]
10. Yu, Y.; Song, X.; Zhang, Y.; Zheng, F.; Liu, L. Impact of reclaimed water in the watercourse of Huai River on groundwater from Chaobai River basin, Northern China. *Front. Earth Sci.* **2017**, *11*, 643–659. [CrossRef]
11. Iwane, T.; Urase, T.; Yamamoto, K. Possible impact of treated wastewater discharge on incidence of antibiotic resistant bacteria in river water. *Water Sci. Technol. J. Int. Assoc. Water Pollut. Res.* **2001**, *43*, 91–99. [CrossRef]
12. Qin, C.; Liu, H.; Liu, L.; Smith, S.; Sedlak, D.L.; Gu, A.Z. Bioavailability and characterization of dissolved organic nitrogen and dissolved organic phosphorus in wastewater effluents. *Sci. Total Environ.* **2015**, *511*, 47–53. [CrossRef]
13. Gibbs, R.J. Mechanisms controlling world water chemistry. *Science* **1970**, *170*, 1088–1090. [CrossRef]
14. Meybeck, M. Global occurrence of major elements in rivers. *Treatise Geochem.* **2003**, *5*, 207–223.
15. Qu, B.; Sillanpää, M.; Zhang, Y.; Guo, J.; Wahed, M.S.M.A.; Kang, S. Water chemistry of the headwaters of the Yangtze River. *Environ. Earth Sci.* **2015**, *74*, 1–16. [CrossRef]
16. Zhu, B.; Yu, J.; Qin, X.; Rioual, P.; Xiong, H. Climatic and geological factors contributing to the natural water chemistry in an arid environment from watersheds in northern Xinjiang, China. *Geomorphology* **2012**, *153–154*, 102–114. [CrossRef]
17. Cerling, T.E.; Pederson, B.L.; Von Damm, K.L. Sodium-calcium ion exchange in the weathering of shales: Implications for global weathering budgets. *Geology* **1989**, *17*, 552. [CrossRef]
18. Liu, B.; Liu, C.Q.; Zhang, G.; Zhao, Z.Q.; Li, S.L.; Hu, J.; Ding, H.; Lang, Y.C.; Li, X.D. Chemical weathering under mid-to cool temperate and monsoon-controlled climate: A study on water geochemistry of the Songhuajiang River system, northeast China. *Appl. Geochem.* **2013**, *31*, 265–278. [CrossRef]
19. Grasby, S.E.; Hutcheon, I.; Mcfarland, L. Surface-water-groundwater interaction and the influence of ion exchange reactions on river chemistry. *Geology* **1999**, *27*, 223. [CrossRef]
20. Azhar, S.C.; Aris, A.Z.; Yusoff, M.K.; Ramli, M.F.; Juahir, H. Classification of river water quality using multivariate analysis. *Procedia Environ. Ences* **2015**, *30*, 79–84. [CrossRef]
21. Costa, M.; Gonçalves, A.M. Clustering and forecasting of dissolved oxygen concentration on a river basin. *Stoch. Environ. Res. Risk Assess.* **2010**, *25*, 151–163. [CrossRef]
22. Alberto, W.D.; del Pilar, D.M.; Valeria, A.M.; Fabiana, P.S.; Cecilia, H.A.; de los Ángeles, B.M. Pattern recognition techniques for the evaluation of spatial and temporal variations in water quality. a case study Suquía River Basin (Córdoba–Argentina). *Water Res.* **2001**, *35*, 2881–2894. [CrossRef]

23. Rong, Y. Statistical methods and pitfalls in environmental data analysis. *Environ. Forensics* **2000**, *1*, 213–220. [CrossRef]
24. Kaiser, H.F. The varimax criteria for analytical rotation in factor analysis. *Psychometrika* **1958**, *23*, 187–200. [CrossRef]
25. Mazlum, N.; Özer, A.; Mazlum, S. Interpretation of water quality data by principal components analysis. *J. Eng. Environ. Sci.* **1999**, *23*, 19–26.
26. Zhang, A.; Ye, C.; Li, Y.; Xie, Z. *Groundwater in Beijing*; China Land Press: Beijing, China, 2008. (In Chinese)
27. Zhang, T.; Li, M.; Yang, Q.; Yu, F.; Qian, T. Scheme of water delivery in the water transfer project from Wenyu River to Chaobai River. *South. North Water Divers. Water Sci. Technol.* **2012**, *10*, 118–120. (In Chinese)
28. SEPA (State Environmental Protection Administration). *Water and Wastewater Monitoring and Analysis Methods (Version 4)*; China Environmental Science Press: Beijing, China, 2002. (In Chinese)
29. Norusis, M. *SPSS 16.0 Guide to Data Analysis*; Prentice Hall Press: Upper Saddle River, NJ, USA, 2008.
30. Mujica, L.E.; Vehí, J.; Ruiz, M.; Verleysen, M.; Staszewski, W.; Worden, K. Multivariate statistics process control for dimensionality reduction in structural assessment. *Mech. Syst. Signal. Process.* **2008**, *22*, 155–171. [CrossRef]
31. Reimann, C.; Filzmoser, P. Normal and lognormal data distribution in geochemistry death of a myth. Consequences for the statistical treatment of geochemical and environmental data. *Environ. Geol.* **2000**, *39*, 1001–1014. [CrossRef]
32. Parkhurst, D.L. User's guide to PHREEQC a computer program for speciation, batch-reaction, one-dimensional transport, and inverse geochemical calculations SuDoc I 19.42/4. *U.S. Geol. Surv. Water Resour. Investig. Rep.* **1999**, *312*. [CrossRef]
33. Shaki, A.A.; Adeloye, A.J. Evaluation of quantity and quality of irrigation water at Gadowa irrigation project in Murzuq basin, southwest Libya. *Agric. Water Manag.* **2006**, *84*, 193–201. [CrossRef]
34. Ayers, R.S.; Westcot, D.W. *Water Quality for Agriculture*; FAO: Rome, Italy, 1985.
35. Kuenzler, E.J.; Stone, K.L.; Albert, D.B. *Phytoplankton Uptake and Sediment Release of Nitrogen and Phosphorus in the Chowan River, North Carolina*; Water Resources Research Institute of the University of North Carolina: Raleigh, NC, USA, 1982.
36. Quiblier, C.; Leboulanger, C.; Sane, S.; Dufour, P. Phytoplankton growth control and risk of cyanobacterial blooms in the lower Senegal River delta region. *Water Res.* **2008**, *42*, 1023–1034. [CrossRef]
37. Deletic, A. The first flush load of urban surface runoff. *Water Res.* **1998**, *32*, 2462–2470. [CrossRef]
38. Vrebos, D.; Beauchard, O.; Meire, P. The impact of land use and spatial mediated processes on the water quality in a river system. *Sci. Total Environ.* **2017**, *601*, 365–373. [CrossRef]
39. Strauss, E.A.; Richardson, W.B.; Bartsch, L.A.; Cavanaugh, J.C.; Bruesewitz, D.A.; Imker, H.; Heinz, J.A.; Soballe, D.M. Nitrification in the Upper Mississippi River: Patterns, controls, and contribution to the NO_3−budget. *J. North Am. Benthol. Soc.* **2004**, *61*, 1102–1112. [CrossRef]
40. Brion, N.; Billen, G. Wastewater as a source of nitrifying bacteria in river systems: The case of the River Seine downstream from Paris. *Water Res.* **2000**, *34*, 3213–3221. [CrossRef]
41. Zhu, B.; Yu, J.; Qin, X.; Rioual, P.; Zhang, Y.; Liu, Z.; Yan, M.; Li, H.; Ren, X.; Xiong, H. Identification of rock weathering and environmental control in arid catchments (northern Xinjiang) of Central Asia. *J. Asian Earth Sci.* **2013**, *66*, 277–294. [CrossRef]
42. Garcia-Ruiz, R.; Pattinson, S.N.; Whitton, B.A. Denitrification in river sediments: Relationship between process rate and properties of water and sediment. *Freshw. Biol.* **1998**, *39*, 467–476. [CrossRef]
43. Grischek, T.; Hiscock, K.M.; Metschies, T.; Dennis, P.F.; Nestler, W. Factors affecting denitrification during infiltration of river water into a sand and gravel aquifer in Saxony, Germany. *Water Res.* **1998**, *32*, 450–460. [CrossRef]
44. Jia, Z.; Liu, T.; Xia, X.; Xia, N. Effect of particle size and composition of suspended sediment on denitrification in river water. *Sci. Total Environ.* **2016**, *541*, 934–940. [CrossRef]
45. Cohen, R.R.H. Biochemical oxygen demand and algae: Fractionation of phytoplankton and nonphytoplankton respiration in a large river. *Water Resour. Res.* **1990**, *26*, 671–678. [CrossRef]
46. Gelda, R.K.; Effler, S.W. A river water quality model for chlorophyll and dissolved oxygen that accommodates Zebra Mussel metabolism. *Water Qual. Ecosyst. Model.* **2000**, *1*, 271–309. [CrossRef]

47. Zhou, W.; Yuan, X.; Long, A.; Huang, H.; Yue, W. Different hydrodynamic processes regulated on water quality (nutrients, dissolved oxygen, and phytoplankton biomass) in three contrasting waters of Hong Kong. *Environ. Monit. Assess.* **2014**, *186*, 1705–1718. [CrossRef]
48. Huang, J.; Yin, H.; Chapra, S.C.; Zhou, Q. Modelling dissolved oxygen depression in an urban river in China. *Water* **2017**, *9*, 520. [CrossRef]
49. Kotovshchikov, A.V.; Dolmatova, L.A. Dynamics of Chlorophyll a content in the Ob River and its relationship with abiotic factors. *Inland Water Biol.* **2018**, *11*, 21–28. [CrossRef]
50. Abonyi, A.; Ács, É.; Hidas, A.; Grigorszky, I.; Várbíró, G.; Borics, G.; Kiss, K.T. Functional diversity of phytoplankton highlights long-term gradual regime shift in the middle section of the Danube River due to global warming, human impacts and oligotrophication. *Freshw. Biol.* **2018**. [CrossRef]
51. Craig, H.; Gordon, L.I. Deuterium and Oxygen 18 Variations in the Ocean and Marine Atmosphere. Available online: https://www.worldcat.org/title/deuterium-and-oxygen-18-variations-in-the-ocean-and-the-marine-atmosphere/oclc/8019537 (accessed on 12 September 2020).
52. Craig, H.; Gordon, L.I.; Horibe, Y. Isotopic exchange effects in the evaporation of water: 1. Low-temperature experimental results. *J. Geophys. Res.* **1963**, *68*, 5079–5087. [CrossRef]
53. Craig, H. Isotopic variations in meteoric waters. *Science* **1961**, *133*, 1702–1703. [CrossRef]
54. Wang, Y.; Li, X.; Yao, L.; Zhao, Y.; Pan, Y. Variation of pH and chemical composition of precipitation by multi2step sampling in summer of Beijing 2007. *Environ. Sci.* **2009**, *30*, 2715–2721. (In Chinese)
55. Kuypers, M.M.; Marchant, H.K.; Kartal, B. The microbial nitrogen-cycling network. *Nat. Rev. Microbiol.* **2018**, *16*, 263. [CrossRef]
56. Yu, Y.; Ma, M.; Zheng, F.; Liu, L.; Zhao, N.; Li, X.; Yang, Y.; Guo, J. Spatio-temporal variation and controlling factors of water quality in Yongding river replenished by reclaimed water in Beijing, North China. *Water* **2017**, *9*, 453. [CrossRef]
57. David, A.; Tournoud, M.-G.; Perrin, J.-L.; Rosain, D.; Rodier, C.; Salles, C.; Bancon-Montigny, C.; Picot, B. Spatial and temporal trends in water quality in a Mediterranean temporary river impacted by sewage effluents. *Environ. Monit. Assess.* **2013**, 2517–2534. [CrossRef]
58. Atwebembeire, J.; Andama, M.; Yatuha, J.; Lejju, J.B.; Rugunda, G.K.; Bazira, J. The physico-chemical quality of effluents of selected sewage treatment plants draining into River Rwizi, Mbarara Municipality, Uganda. *J. Water Resour. Prot.* **2019**, *11*, 23–36. [CrossRef]
59. Marei, A.; Khayat, S.; Weise, S.; Ghannam, S.; Sbaih, M.; Geyer, S. Estimating groundwater recharge using the chloride mass-balance method in the West Bank, Palestine. *Hydrol. Sci. J.* **2010**, *55*, 780–791. [CrossRef]
60. Selim, H.M.; Schulin, R.; Flühler, H. Transport and ion exchange of calcium and magnesium in an aggregated soil. *Soil Sci. Soc. Am. J.* **1987**, *51*, 876. [CrossRef]
61. Reid, J.; MacLeod, D.; Cresser, M.S. Factors affecting the chemistry of precipitation and river water in an upland catchment. *J. Hydrol.* **1981**, *50*, 129–145. [CrossRef]
62. Seanego, K.G.; Moyo, N.A.G. The effect of sewage effluent on the physico-chemical and biological characteristics of the Sand River, Limpopo, South Africa. *Phys. Chem. Earth Parts A B C* **2013**, *66*, 75–82. [CrossRef]
63. Perkins, R.G.; Underwood, G.J.C. The potential for phosphorus release across the sediment–water interface in an eutrophic reservoir dosed with ferric sulphate. *Water Res.* **2001**, *35*, 1399–1406. [CrossRef]
64. Kim, L.H.; Choi, E.; Stenstrom, M.K. Sediment characteristics, phosphorus types and phosphorus release rates between river and lake sediments. *Chemosphere* **2003**, *50*, 53–61. [CrossRef]
65. Liu, J.; Song, X.; Fu, G.; Liu, X.; Zhang, Y.; Han, D. Precipitation isotope characteristics and climatic controls at a continental and an island site in Northeast Asia. *Clim. Res.* **2011**, *49*, 29–44. [CrossRef]
66. Wang, L.; Caylor, K.K.; Villegas, J.C.; Barron-Gafford, G.A.; Breshears, D.D.; Huxman, T.E. Partitioning evapotranspiration across gradients of woody plant cover: Assessment of a stable isotope technique. *Geophys. Res. Lett.* **2010**, 37. [CrossRef]
67. Song, X.; Tang, Y.; Zhang, Y.; Ma, Y.; Han, D.; Bu, H.; Yang, L.; Liu, F. Using stable isotopes to study vapor transport of continuous precipitation in Beijing. *Adv. Water Sci.* **2017**, *28*, 387–495. (In Chinese)
68. Fan, B.L.; Zhao, Z.Q.; Tao, F.X.; Liu, B.J.; Tao, Z.H.; Gao, S.; Zhang, L.H. Characteristics of carbonate, evaporite and silicate weathering in Huanghe River basin: A comparison among the upstream, midstream and downstream. *J. Asian Earth Sci.* **2014**, *96*, 17–26. [CrossRef]

69. Smolders, A.J.P.; Hudson-Edwards, K.A.; Velde, G.V.d.; Roelofs, J.G.M. Controls on water chemistry of the Pilcomayo river (Bolivia, South-America). *Appl. Geochem.* **2004**, *19*, 1745–1758. [CrossRef]
70. Li, J.; Yuan, G.L.; Deng, X.R.; Jing, X.M.; Sun, T.H.; Lang, X.X.; Wang, G.H. Major ion geochemistry of the Nansihu Lake basin rivers, North China: Chemical weathering and anthropogenic load under intensive industrialization. *Environ. Earth Sci.* **2016**, *75*, 453. [CrossRef]
71. Reddy, A.G.S.; Saibaba, B.; Sudarshan, G. Hydrogeochemical characterization of contaminated groundwater in Patancheru industrial area, southern India. *Environ. Monit. Assess.* **2012**, *184*, 3557. [CrossRef] [PubMed]
72. Singh, C.K.; Shashtri, S.; Mukherjee, S. Integrating multivariate statistical analysis with GIS for geochemical assessment of groundwater quality in Shiwaliks of Punjab, India. *Environ. Earth Sci.* **2010**, *62*, 1387–1405. [CrossRef]
73. Moon, S.; Huh, Y.; Qin, J.; Pho, N.V. Chemical weathering in the Hong (Red) River basin: Rates of silicate weathering and their controlling factors. *Geochim. Et Cosmochim. Acta* **2007**, *71*, 1411–1430. [CrossRef]
74. Jahangir, M.M.; Khalil, M.I.; Johnston, P.; Cardenas, L.M.; Hatch, D.J.; Butler, M.; Barrett, M.; O'flaherty, V.; Richards, K.G. Denitrification potential in subsoils: A mechanism to reduce nitrate leaching to groundwater. *Agric. Ecosyst. Environ.* **2012**, *147*, 13–23. [CrossRef]
75. Gomez-Velez, J.D.; Harvey, J.W.; Cardenas, M.B.; Kiel, B. Denitrification in the Mississippi River network controlled by flow through river bedforms. *Nat. Geosci.* **2015**, *8*, 941–945. [CrossRef]
76. Zhao, L.; Delatolla, R.; Mohammadian, A. Nitrification Kinetics & Modified Model for the Rideau River, Canada. *Water Qual. Res. J. Can.* **2013**, *48*, 192–201.
77. Radwan, D.M.; Willems, D.P.; El Sadek, D.A.; Berlamont, P.J. Modelling of dissolved oxygen and biochemical oxygen demand in river water using a detailed and a simplified model. *Int. J. River Basin Manag.* **2003**, *1*, 97–103. [CrossRef]
78. Yang, J.; Trela, J.; Plaza, E.; Wahlberg, O.; Levlin, E. Oxidation-reduction potential (ORP) as a control parameter in a single-stage partial nitritation/anammox process treating reject water. *J. Chem. Technol. Biotechnol.* **2016**, *91*, 2582–2589. [CrossRef]
79. Tromans, D. Temperature and pressure dependent solubility of oxygen in water: A thermodynamic analysis. *Hydrometallurgy* **1998**, *48*, 327–342. [CrossRef]
80. Weissenbacher, N.; Loderer, C.; Lenz, K.; Mahnik, S.N.; Wett, B.; Fuerhacker, M. NOx monitoring of a simultaneous nitrifying–denitrifying (SND) activated sludge plant at different oxidation reduction potentials. *Water Res.* **2007**, *41*, 397–405. [CrossRef] [PubMed]
81. Mortazavi, B.; Iverson, R.L.; Landing, W.M.; Lewis, F.G.; Huang, W.R. Control of phytoplankton production and biomass in a river-dominated estuary: Apalachicola Bay, Florida, USA. *Mar. Ecol. Prog.* **2000**, *198*, 19–31. [CrossRef]
82. Redfield, A.C.; Ketchum, B.H.; Richards, F.A. The influence of organisms on the composition of sea-water. In *The Sea Water*; Interscience Publishers: New York, NY, USA, 1963.
83. Bulgakov, N.G.; Levich, A.P. The nitrogen: Phosphorus ratio as a factor regulating phytoplankton community structure. *Arch. Hydrobiol.* **1999**, *146*, 3–22. [CrossRef]
84. MHURD, C. *The Reuse of Urban Recycling Water—Water Quality Standard For Scenic Environment Use (Gb/T 18921–2019)*; Chinese Specification Press: Beijing, China, 2020; p. 5. (In Chinese)
85. EPA, C. *Surface Water Environmental Quality Standard (GB3838-2002)*; China Environmental Science Press: Beijing, China, 2002. (In Chinese)
86. Richards, L.A. *Diagnosis And Improvements of Saline And Alkali Soils*; National Agricultural Library: Washington, DC, USA, 1954.
87. Brown, C.D.; Canfield, D.E.; Bachmann, R.W.; Hoyer, M.V. Seasonal patterns of chlorophyll, nutrient concentrations and Secchi disk transparency in Florida lakes. *Lake Reserv. Manag.* **1998**, *14*, 60–76. [CrossRef]
88. Wang, X.J.; Liu, R.M. Spatial analysis and eutrophication assessment for chlorophyll a in Taihu Lake. *Environ. Monit. Assess.* **2005**, *101*, 167.